Computation of the temperature dependence of the heat capacity of complex molecular systems using random color noise

Sahin Buyukdagli,[1] Alexander V. Savin,[2] and Bambi Hu[1,3]
[1]*Department of Physics and Centre for Nonlinear Studies, Hong Kong Baptist University, Hong Kong, China*
[2]*Semenov Institute of Chemical Physics, Russian Academy of Sciences, Moscow 119991, Russia*
[3]*Department of Physics, University of Houston, Houston, Texas 77204-5005, USA*
(Received 3 April 2008; revised manuscript received 14 October 2008; published 18 December 2008)

We propose a method for computing the temperature dependence of the heat capacity in complex molecular systems. The proposed scheme is based on the use of the Langevin equation with low-frequency color noise. We obtain the temperature dependence of the correlation time of random noises, which enables us to model the partial thermalization of high-frequency vibrations. This purely quantum effect is responsible for the decreasing behavior of the specific heat $c(T)$ in the low-temperature regime. By applying the method to carbon nanotubes and polyethylene molecules, we show that the consideration of the color noise in the Langevin equation allows us to reproduce the temperature evolution of the specific heat with a good accuracy.

DOI: 10.1103/PhysRevE.78.066702 PACS number(s): 02.70.Ns, 05.10.Gg, 65.80.+n

The pronounced temperature dependence of the specific heat $c(T)$ in molecular systems is a pure quantum effect. It is well known that in the absence of any critical point, the increase of the temperature is accompanied by a smooth rise of the specific heat $c(T)$, while by decreasing the temperature, $c(T)$ tends to zero. The first explanation for this quantum phenomenon was given by Einstein a century ago [1].

From the point of view of the classical physics, the decreasing tendency of the specific heat looks like an effect of "partial freezing" of high-frequency vibrational modes, while low-frequency vibrations would be fully excited. This incomplete picture is of course due to the inadequacy of the classical physics to provide a self-consistent explanation for this effect. In fact, the use of the usual Langevin equation with white noise leads to a uniform thermalization of all modes, and the specific heat is practically insensitive to the temperature (in classical physics, any temperature dependence of the thermal capacity results from nonlinearity effects). On the other hand, it is possible to mimic the "partial thermalization" effect in the framework of the Langevin description if one considers, instead of a white noise, a low-frequency color noise with a temperature-dependent frequency spectrum. To this end, it is enough to introduce a random noise with a finite correlation time $t_c>0$ during which the noise "remembers" its last realization. In this study, we obtain the temperature dependence of this correlation time, which allows a correct modeling of the "partial thermalization" of vibrations in the system. A thorough discussion about the relation between the white noise and the correlated noise can be found in [2,3].

The paper is organized as follows. We consider in Sec. I a harmonic oscillator and investigate its dynamics described by the Langevin equation with color noise. We obtain the temperature dependence of the correlation time of random noises, which enables us to efficiently model the "partial thermalization" of high-frequency vibrations. We next evaluate in Sec. II the effect of nonlinearities on the accuracy of our computational method, and we propose a general scheme to compute the heat capacity for many-body systems using a color noise. Sections III and IV are devoted to the application of the proposed scheme to a Hamiltonian carbon nanotube model and a polyethylene macromolecule, respectively. It is shown in these sections that the temperature evolution of the specific heat computed with the Langevin equation with color noise agrees well with the result obtained from a direct quantum-mechanical calculation.

I. THE LANGEVIN EQUATION

The thermalization of the mode of frequency Ω is described by the Langevin equation

$$\ddot{u} + \Omega^2 u + \Gamma \dot{u} = \xi(t)/\mu, \tag{1}$$

where u is the coordinate of the vibration; damping $\Gamma = 1/t_r$, and t_r is the relaxation time; μ is the reduced mass of the mode; $\xi(t)$ is a normally distributed random force that describes the interaction of the mode with the thermal bath of temperature T and the autocorrelation function

$$\langle \xi(t)\xi(t') \rangle = 2\mu\Gamma k_B T \varphi(t-t')$$

[the dimensionless function $\varphi(t)$ is normalized as $\int_{-\infty}^{+\infty}\varphi(t)dt = 1$], where k_B is the Boltzmann constant.

At thermal equilibrium, the averaged energy of thermal vibrations is defined by the relation

$$E = \lim_{\tau\to\infty} \frac{1}{\tau}\int_0^\tau \frac{\mu}{2}(\dot{u}^2 + \Omega^2 u^2)dt$$
$$= \int_0^{+\infty} \mu(\omega^2 + \Omega^2)|H(\omega)|^2 F(\omega)d\omega, \tag{2}$$

where $H(\omega) = [\mu(\Omega^2 - \omega^2 + i\omega\Gamma)]^{-1}$ is the transmission function and $F(\omega)$ is the Fourier transform of the autocorrelation function of the random force,

$$F(\omega) = \frac{1}{2\pi}\int_{-\infty}^{+\infty} \langle \xi(t)\xi(0)\rangle \exp\{-i\omega t\}dt$$

$$= \frac{\mu\Gamma k_B T}{\pi}\int_{-\infty}^{+\infty} \varphi(t)\exp\{-i\omega t\}dt. \quad (3)$$

Thus, $E=K+P$, where the averaged kinetic energy is defined by the relation

$$K = \lim_{\tau\to\infty}\frac{1}{\tau}\int_0^\tau \frac{1}{2}\mu\dot{u}^2 dt = 2k_B T\Gamma\int_0^{+\infty}\frac{\omega^2\mathcal{F}(\omega)d\omega}{(\Omega^2-\omega^2)^2+\omega^2\Gamma^2} \quad (4)$$

and the averaged potential energy is given by

$$P = \lim_{\tau\to\infty}\frac{1}{\tau}\int_0^\tau \frac{1}{2}\mu\Omega^2 u^2 dt = 2k_B T\Gamma\int_0^{+\infty}\frac{\Omega^2\mathcal{F}(\omega)d\omega}{(\Omega^2-\omega^2)^2+\omega^2\Gamma^2}, \quad (5)$$

where $\mathcal{F}(\omega)$ is the Fourier transform of the dimensionless autocorrelation function $\varphi(t)$,

$$\mathcal{F}(\omega) = \frac{1}{2\pi}\int_{-\infty}^{+\infty}\varphi(t)\exp\{-i\omega t\}dt.$$

For a δ-correlated random force (the case of the white noise), $\varphi(t)=\delta(t)$ and $\mathcal{F}(\omega)=1/2\pi$. The integrals (4) and (5) can be easily calculated by a contour integration. The energy $E=K=k_BT/2$ at $\Omega=0$ and $E=K+P=k_BT$, $K=P=k_BT/2$ for frequency $\Omega>0$.

For an exponentially correlated random force (the case of low-frequency color noise), $\varphi(t)=\frac{1}{2}\lambda\exp-|\lambda t|$ and $\mathcal{F}(\omega)=\lambda^2/2\pi(\omega^2+\lambda^2)$, where $\lambda=1/t_c$ and t_c is the correlation time of the random force. In this case, the integrals (4) and (5) can also be calculated by a contour integration. The averaged kinetic energy $K=k_BTf_K(\Omega,\Gamma,\lambda)/2$ and the averaged potential energy $P=k_BTf_P(\Omega,\Gamma,\lambda)/2$ with f_K and f_P defined by

$$f_K(\Omega,\Gamma,\lambda) = \lambda^2/(\lambda^2+\lambda\Gamma+\Omega^2), \quad (6)$$

$$f_P(\Omega,\Gamma,\lambda) = \frac{\lambda^2(\Omega^2+\lambda^2-\Gamma^2)+\lambda\Gamma\Omega^2}{(\Omega^2+\lambda^2)^2-\Gamma^2\lambda^2}. \quad (7)$$

Let us note at this point that in the limit $\Omega\to 0$, one gets $f_K=\lambda^2/(\lambda^2+\lambda\Gamma)$, $f_P=1$. In the present work, we kept the numerical value of the damping Γ small enough. In this case (the limit $\Gamma\to 0$), formulas (6) and (7) take the simple form $f_K=f_P=\lambda^2/(\lambda^2+\Omega^2)$.

In the case of an harmonic oscillator, the Langevin equation with white noise describes thermal vibrations of harmonic modes in the classical approximation, where the mean energy obeys $E=k_BT$. If one considers instead a quantum harmonic oscillator $H=\hbar\Omega(B^+B+\frac{1}{2})$, where $\hbar$ is the Planck constant, and B^+ and B represent creation and annihilation operators, the mean energy of thermal vibrations is given by

$$E(\Omega,T) = \frac{\hbar\Omega}{\exp(\hbar\Omega/k_BT)-1}+\frac{1}{2}\hbar\Omega. \quad (8)$$

The heat capacity of the oscillator is defined by $c(\Omega,T)=dE(\Omega,T)/dT=k_BF_E(\Omega,T)$, where the Einstein function behaves according to

$$F_E(\Omega,T) = \left(\frac{\hbar\Omega}{k_BT}\right)^2\frac{\exp(\hbar\Omega/k_BT)}{[\exp(\hbar\Omega/k_BT)-1]^2}.$$

For $T\to\infty$, the Einstein function $F_E(\Omega,T)\to 1$, while in the limit $T\to 0$, we get $F_E(\Omega,T)\to 0$. Consequently, at high temperatures, the specific heat behaves as $c(\Omega,T)\approx k_B$, and at low temperatures one has $c(\Omega,T)\approx 0$. For this reason, in the low-temperature regime defined by $T<T_E=\hbar\Omega/k_B$, vibrations of the quantum oscillator are "partially frozen." Consequently, a classical description of thermal vibrations is valid exclusively in the high-temperature regime $T>T_E$, where the Einstein temperature T_E is defined by $F_E(\Omega,T_E)=e/(e-1)^2=0.920\,673\,5$.

If we drop the energy of vacuum vibrations $\hbar\Omega/2$, the thermalization of the quantum oscillator can be characterized by the function

$$G(\Omega,T) = [E(\Omega,T)-\hbar\Omega/2]/k_BT = \frac{\hbar\Omega/k_BT}{\exp(\hbar\Omega/k_BT)-1}.$$

In the limit $T\to 0$, the thermalization coefficient $G(\Omega,T)\to 0$, while at $T=T_E$ the function $G(\Omega,T_E)=1/(e-1)=0.581\,976\,7$, and in the limit $T\to\infty$, we have $G(\Omega,T)\to 1$. Hence for temperatures $T>0$, vibrations with frequency $\Omega>\Omega_E(T)=k_BT/\hbar$ will be "partly frozen." We can thus conclude that it is incorrect to model thermal fluctuations of these modes using the Langevin equation with white noise.

As we stated at the beginning of this paper, the partial thermalization of high-frequency vibrations and the total thermalization of low-frequency modes can be realized if one uses a Langevin equation with color noise, which consists of low-frequency components of the white noise. But it is necessary to consider in this case the temperature dependence of the noise correlation functions. For an exponentially correlated random noise, this dependence can be deduced from the relation

$$G(\Omega_E(T),T) \approx [f_K(\Omega_E(T),\Gamma,\lambda)+f_P(\Omega_E(T),\Gamma,\lambda)]/2.$$

In the limit $\Gamma\ll\Omega_E(T)=k_BT/\hbar$, using Eqs. (6) and (7), the last equation can be expressed in the simple form

$$\frac{\lambda^2}{\lambda^2+(k_BT/\hbar)^2} = \frac{1}{e-1}. \quad (9)$$

Equation (9) yields the following linear temperature dependence of the correlation coefficient:

$$\lambda = 1/t_c = k_BT/\hbar\sqrt{e-2}. \quad (10)$$

It follows from Eq. (10) that the description of the partial thermalization of high-frequency vibrations with the use of the Langevin equation (1) becomes possible if we introduce a correlation time t_c that is inversely proportional to the temperature T of the thermal bath, i.e.,

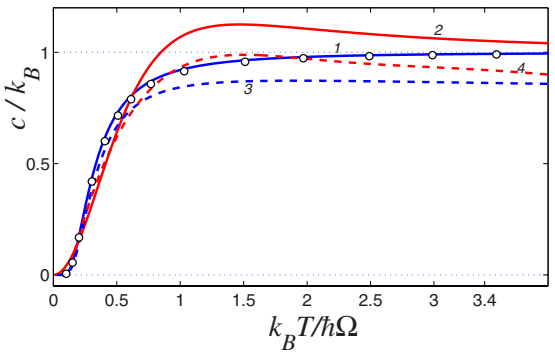

FIG. 1. (Color online) Temperature dependence of the heat capacity of the quantum harmonic (curve 1) and anharmonic oscillator (curve 3), classical harmonic (curve 2), and anharmonic oscillator (curve 4) obtained from the Langevin equation with color noise (Ω is the frequency of the oscillator and the anharmonicity parameter is chosen as β=0.1). Open symboles denote the heat capacity computed according to the spectral density equation (38).

$$t_c = \hbar\sqrt{e-2}/k_B T. \tag{11}$$

The time correlated color noise can be inserted in the Langevin description if one replaces the Langevin equation (1) by the system of two equations,

$$\ddot{u} = -\Omega^2 u - \Gamma\dot{u} + \xi(t)/\mu, \tag{12}$$

$$\dot{\xi} = [\eta(t) - \xi(t)]/t_c, \tag{13}$$

where $\eta(t)$ stands for the white noise generator, normalized according to

$$\langle \eta(t)\eta(t')\rangle = 2\mu\Gamma k_B T\delta(t-t'),$$

and t_c is the correlation time whose temperature dependence is determined by Eq. (11).

Figure 1 compares the specific heat of a quantum harmonic oscillator and a classical oscillator whose dynamics is described by Langevin equations with color noise (12) and (13). It is clear that the introduction of the color noise does not allow us to reproduce the temperature dependence of the quantum oscillator exactly. This is mainly due to the well known inadequacy of a classical description to describe zero vibrations (ground-state fluctuations). The figure nevertheless shows that the use of the color noise yields a qualitatively correct behavior of the heat capacity, that is, in the limit $T\to 0$ the specific heat $c\to 0$, and for $T\to\infty$ one has $c\to k_B$ (with the increase of the temperature, the correlation time tends to zero and the color noise becomes a white noise). Most importantly, we notice that there is a good agreement between the exact quantum result and the modified Langevin description at low temperatures $T<T_E$ where quantum effects dominate.

We have shown that by using the Langevin equation with color noise, one can obtain a qualitatively correct picture for the temperature evolution of the specific heat in the case of a harmonic oscillator. The presence of nonlinearities in the system will be considered in the next section.

II. THE EFFICIENCY OF THE PROPOSED SCHEME IN THE PRESENCE OF NONLINEARITIES

As is well known, anharmonicities are always present in physical systems, and the validity of the harmonic approximation, which consists in representing the building blocks of a condensed system by linear oscillators, is usually restricted to very low energy regimes. The anharmonic intermolecular forces may result either from the nonlinearity of the individual oscillators or from their nonlinear mutual interaction. The natural question arises whether the Langevin equation with color noise can be used in the presence of nonlinearities in the system. As a first attempt to answer this question, let us consider a nonlinear oscillator whose dimensionless Hamiltonian is given by

$$H = \frac{1}{2}\dot{u}^2 + \frac{1}{2}u^2 + \frac{1}{4}\beta u^4. \tag{14}$$

The corresponding Langevin equation with color noise can be written in the form

$$\ddot{u} = -u - \beta u^3 - \Gamma\dot{u} + \xi(t),$$

$$\dot{\xi} = [\eta(t) - \xi(t)]/t_c,$$

$$\langle \eta(t)\eta(t')\rangle = 2\Gamma T\delta(t-t'), \tag{15}$$

where T is the dimensionless temperature, the friction coefficient Γ=0.01, and the correlation time $t_c=\sqrt{e-2}/T$.

The numerical integration of the set of equations of motion (15) yields the mean energy $E=\langle H\rangle$ of the anharmonic oscillator as a function of T. Then the specific heat is computed from $c(T)=dE/dT$.

In order to check the accuracy of the modified Langevin equation, we obtained equally the specific heat of this oscillator by computing numerically the exact eigenvalues E_n of the quartic Hamiltonian (14). The diagonalization of the Hamiltonian matrix was performed in the basis of the harmonic oscillator. The obtained eigenvalues were then used to find the partition function and the specific heat from the well-known relations

$$Z(T) = \sum_n e^{-E_n/T},$$

$$F(T) = -T\ln(Z),$$

$$c(T) = -T\frac{d^2F}{dT^2}. \tag{16}$$

We compare in Fig. 1 the result of the numerical simulation to that obtained from the quantum statistical calculation (curve 3 and 4) for β=0.1. We notice that the nonlinearity effects are indistinguishable within the accuracy of the proposed method.

In order to examine the effect of nonlinearities present in mutual interactions between vibrational modes, let us consider now the case of two linear oscillators with a dimensionless Hamiltonian

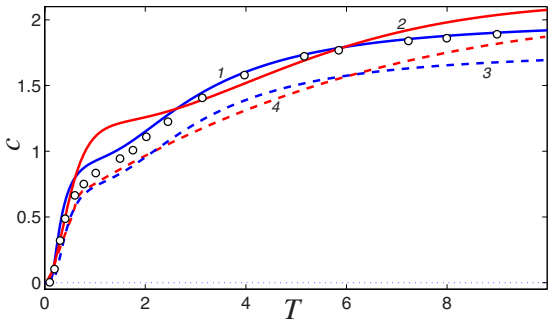

FIG. 2. (Color online) Temperature dependence of the heat capacity for the system of two coupled linear oscillators (with frequencies $\omega_1=1$, $\omega_2=10$) obtained from a direct quantum-mechanical calculation (curves 1,3) and the Langevin equation with color noise (curves 2,4). Solid lines correspond to decoupled oscillators ($\beta=0$) and dashed lines to a coupling $\beta=1$. Open symbols denote the heat capacity computed according to the spectral density equation (38).

$$H=\frac{1}{2}(\dot{u}_1^2+\dot{u}_2^2+\omega_1^2u_1^2+\omega_2^2u_2^2)+\frac{1}{4}\beta(u_1-u_2)^4, \quad (17)$$

where the variable u_i describes the dynamics of the ith oscillator ($i=1,2$), ω_i is the frequency of the same mode, and the parameter β sets the strength of the nonlinear interaction between the two oscillators. For this two-body Hamiltonian, the system of Langevin equations with color noise takes the form

$$\ddot{u}_1=-\omega_1u_1+\beta(u_2-u_1)^3-\Gamma\dot{u}_1+\xi_1(t),$$

$$\ddot{u}_2=-\omega_2u_2-\beta(u_2-u_1)^3-\Gamma\dot{u}_2+\xi_2(t),$$

$$\dot{\xi}_1=[\eta_1(t)-\xi_1(t)]/t_c,$$

$$\dot{\xi}_2=[\eta_2(t)-\xi_2(t)]/t_c, \quad (18)$$

where $\eta_i(t)$ stands for the random function that generates white noise with normalization conditions

$$\langle\eta_i(t)\eta_i(t')\rangle=2\Gamma T\delta(t-t'), \quad i=1,2, \quad \langle\eta_1(t)\eta_2(t')\rangle=0.$$

(T is dimensionless temperature, the dissipation coefficient is chosen as $\Gamma=0.01$, and the correlation time is given by $t_c=\sqrt{e-2}/T$.)

It is also possible for this two-body system to obtain the temperature dependence of the specific heat from a purely quantum-mechanical calculation, that is, by diagonalizing the Hamiltonian matrix corresponding to Eq. (17) in the product basis of two harmonic oscillators of frequencies ω_1 and ω_2. The obtained energy levels were then used in Eq. (16) in order to obtain the specific heat.

For the sake of distinctness, we chose $\omega_1=1$ and $\omega_2=10$. The result of the numerical integration of the equations of motion (18) illustrated in Fig. 2 indeed shows that the presence of nonlinearities in the interaction between individual modes improves the precision of the proposed Langevin approach with color noise. To be more precise, for an interaction strength of $\beta=1$, the temperature dependence of $c(T)$ agrees better than the noninteracting case $\beta=0$ with the result obtained from quantum-statistical mechanics.

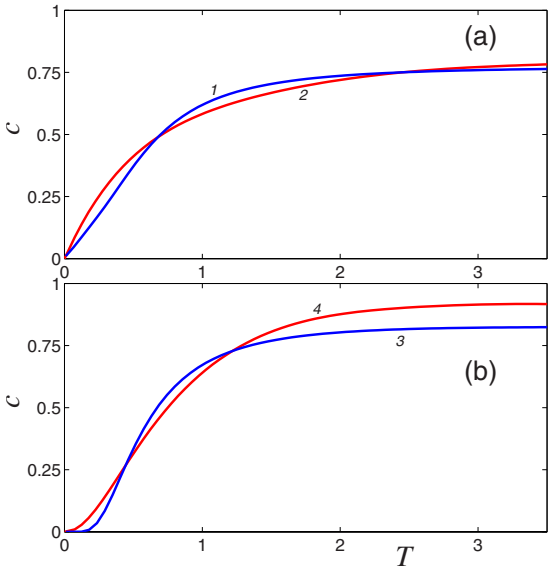

FIG. 3. (Color online) Temperature dependence of the heat capacity for (a) the one-dimensional FPU-β model and (b) the ϕ^4 model, obtained from the first-order variational method (curves 1 and 3) and the Langevin equation with color noise (curves 2 and 4).

We also computed the heat capacity of the previous models according to the spectral density equation (38) that we introduce below. One can see in Figs. 1 and 2 that the result obtained in this way closely follows the exact quantum-mechanical result.

We have so far considered only small molecular systems. In order to check the efficiency of the generalized Langevin method for many-body systems, we will now discuss the calculation of the specific heat for the one-dimensional (1D) Fermi-Pasta-Ulam (FPU) model,

$$H=\sum_i\left\{\frac{p_i^2}{2m}+\frac{K}{2}\delta u_i^2+\frac{\lambda}{4}\delta u_i^4\right\}, \quad (19)$$

and ϕ^4 chain,

$$H=\sum_i\left\{\frac{p_i^2}{2m}+\frac{K}{2}\delta u_i^2+\frac{f_o}{2}u_i^2+\frac{\lambda}{4}u_i^4\right\}, \quad (20)$$

where $K=m=\lambda=f_o=1$ for both models, $\delta u_i=u_i-u_{i-1}$ stands for the interparticle distance, and the index i runs over oscillators.

Figure 3 compares the specific heat of these Hamiltonian chains computed with the generalized Langevin approach to the one obtained from a first-order variational method. A brief description of the variational calculation can be found in the Appendix. The integration of the Langevin equations with color noise was carried out in the same way as the previous small nonlinear models. Both figures clearly show for these highly nonlinear 1D models the sensitive agreement between the Langevin approach and the statistical mechanical calculation.

These examples clearly show that the use of the Langevin equation with color noise can be used as a reasonably accurate tool to compute the specific heat of complex molecular systems that are very difficult to study within the framework of quantum-statistical mechanics. We will now present the scheme for evaluating the temperature dependence of the specific heat for general molecular systems by using a color noise. Let us define the N-dimensional vector $\mathbf{x}=\{x_n\}_{n=1}^N$, which denotes the spatial coordinates of the individual atoms in the system. In terms of these coordinates, the generalized Langevin equation describing the dynamics of the system takes the form

$$\mathbf{M}\ddot{\mathbf{x}} = -\partial H/\partial \mathbf{x} - \Gamma \mathbf{M}\dot{\mathbf{x}} + \Xi, \tag{21}$$

$$\dot{\Xi} = (\Theta - \Xi)/t_c, \tag{22}$$

where $\mathbf{M}$ is the mass matrix of the atoms, H is the Hamiltonian of the system, the dissipation coefficient is given by $\Gamma = 1/t_r$ (t_r is the relaxation time), $\Theta=\{\eta_n\}_{n=1}^N$ is the vector of normally distributed random forces obeying the normalization conditions

$$\langle \eta_n(t_1)\eta_l(t_2)\rangle = 2M_n k_B T \delta_{nl}\delta(t_1 - t_2), \tag{23}$$

and the temperature dependence of the correlation time t_c is still determined by the relation (11). The choice of characteristic times for the integration of the generalized Langevin equations requires some care. In fact, since the formula (11) was obtained in the limit $\Gamma \ll k_B T/\hbar$, the numerical value of the relaxation time should be large enough. It is thus crucial that the fixed value of the relaxation time remains always bigger than the correlation time of random forces in the considered temperature regime. On the other hand, very large values of t_r are not suitable since it would require exceedingly long integration times to drive the system to thermal equilibrium. From a practical point of view, the numerical value $t_r = 1$ ps is adequate since the result remains practically invariant under the increase of this characteristic time.

The proposed scheme will be applied in the next section to a Hamiltonian carbon nanotube model.

III. COMPUTATION OF THE HEAT CAPACITY OF CARBON NANOTUBES

Carbon nanotubes have the peculiarity of behaving as quasi-one-dimensional systems. This characteristic allows us to compute the specific heat of these structures using quantum-statistical tools, and this is what we will exploit in this section in order to check the efficiency of our modified Langevin approach on a concrete molecular system.

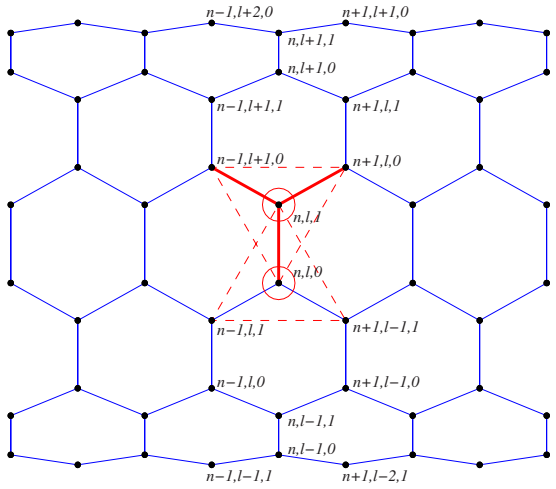

FIG. 4. (Color online) Schematic representation of a carbon nanotube with chirality (m,m) and numbering of atoms in the structure. Thick red lines mark valent bond couplings, thin red arcs mark valent angle couplings, and thin dashed lines show the foundation of two pyramids that form dihedral angles along the valent bonds in the elementary cell (n,l). For this figure, we chose $m=6$.

For the sake of simplicity, we will limit ourselves to the case of a nanotube with index of chirality (m,m). The structure of a carbon nanotube (CNT) with chirality (m,m) (armchair structure) is shown schematically in Fig. 4. The nanotube is characterized by its radius R, the angle shift φ, and the longitudinal step h. The system consists of parallel transversal layers of atoms. In each layer, the nanotube has $2m$ atoms, which form m elementary cells separated by the angular distance $\Delta\phi = 2\pi/m$, so that h defines the alternating longitudinal distances between the transverse layers. Each atom of the CNT can be characterized by three indices (n,l,k), where (n,l) defines an elementary cell ($n=0,\pm 1,\ldots$, $l=1,2,\ldots,m$), and k is the atom number in the cell, $k=0,1$ (see Fig. 4).

The Hamiltonian of the lattice of carbon atoms shown in Fig. 4 can be written in the following general form:

$$\mathcal{H} = \sum_n \sum_{l=1}^m \left[\frac{1}{2} M(\dot{\mathbf{u}}_{n,l,0}^2 + \dot{\mathbf{u}}_{n,l,1}^2) + \mathcal{P}_{n,l} \right], \tag{24}$$

where M is the mass of a carbon atom, $M = 12 \times 1.6603 \times 10^{-27}$ kg, $\mathbf{u}_{n,l,k}=(x_{n,l,k}(t), y_{n,l,k}(t), z_{n,l,k}(t))$ is the radius-vector that defines the position of the carbon atom (n,l,k) at the moment t, and the term $\mathcal{P}_{n,l} \equiv P(\mathbf{u}_{n-1,l,1}, \mathbf{u}_{n-1,l+1,0}, \mathbf{u}_{n,l,0}, \mathbf{u}_{n,l,1}, \mathbf{u}_{n+1,l-1,1}, \mathbf{u}_{n+1,l,0})$ denotes the total potential energy given by a sum of three different types of potentials,

$$\begin{aligned}
\mathcal{P}_{n,l} = {} & V(\mathbf{u}_{n,l,0}, \mathbf{u}_{n,l,1}) + V(\mathbf{u}_{n-1,l+1,0}, \mathbf{u}_{n,l,1}) + V(\mathbf{u}_{n,l,1}, \mathbf{u}_{n+1,l,0}) + U(\mathbf{u}_{n-1,l,1}, \mathbf{u}_{n,l,0}, \mathbf{u}_{n,l,1}) + U(\mathbf{u}_{n+1,l-1,1}, \mathbf{u}_{n,l,0}, \mathbf{u}_{n,l,1}) \\
& + U(\mathbf{u}_{n-1,l,1}, \mathbf{u}_{n,l,0}, \mathbf{u}_{n+1,l-1,1}) + U(\mathbf{u}_{n,l,0}, \mathbf{u}_{n,l,1}, \mathbf{u}_{n-1,l+1,0}) + U(\mathbf{u}_{n,l,0}, \mathbf{u}_{n,l,1}, \mathbf{u}_{n+1,l,0}) + U(\mathbf{u}_{n-1,l+1,0}, \mathbf{u}_{n,l,1}, \mathbf{u}_{n+1,l,0}) \\
& + W(\mathbf{u}_{n,l,1}, \mathbf{u}_{n,l,0}, \mathbf{u}_{n-1,l,1}, \mathbf{u}_{n+1,l-1,1}) + W(\mathbf{u}_{n,l,1}, \mathbf{u}_{n,l,0}, \mathbf{u}_{n+1,l-1,1}, \mathbf{u}_{n-1,l,1}) + W(\mathbf{u}_{n-1,l,1}, \mathbf{u}_{n,l,0}, \mathbf{u}_{n,l,1}, \mathbf{u}_{n+1,l-1,1}) \\
& + W(\mathbf{u}_{n,l,0}, \mathbf{u}_{n,l,1}, \mathbf{u}_{n-1,l+1,0}, \mathbf{u}_{n+1,l,0}) + W(\mathbf{u}_{n,l,0}, \mathbf{u}_{n,l,1}, \mathbf{u}_{n+1,l,0}, \mathbf{u}_{n-1,l+1,0}) + W(\mathbf{u}_{n-1,l+1,0}, \mathbf{u}_{n,l,1}, \mathbf{u}_{n,l,0}, \mathbf{u}_{n+1,l,0}).
\end{aligned} \tag{25}$$

The first three terms describe a change of the deformation energy due to a direct interaction between pairs of atoms with coordinates $\mathbf{u}_1$ and $\mathbf{u}_2$, characterized by the potential $V(\mathbf{u}_1,\mathbf{u}_2)$. The next six terms describe the deformation energy of the angle between the links $\mathbf{u}_1\mathbf{u}_2$ and $\mathbf{u}_2\mathbf{u}_3$, taken into account the potential $U(\mathbf{u}_1,\mathbf{u}_2,\mathbf{u}_3)$. Finally, the next six terms describe the deformation energy associated with a change of the effective angle between the planes $\mathbf{u}_1\mathbf{u}_2\mathbf{u}_3$ and $\mathbf{u}_2\mathbf{u}_3\mathbf{u}_4$, characterized by the potential $W(\mathbf{u}_1,\mathbf{u}_2,\mathbf{u}_3,\mathbf{u}_4)$.

In our numerical simulations, we employ the interaction potentials frequently used in modeling the dynamics of polymer macromolecules [4–6],

$$V(\mathbf{u}_1,\mathbf{u}_2) = D\{\exp[-\alpha(\rho-\rho_0)]-1\}^2, \tag{26}$$

where $\rho=|\mathbf{u}_2-\mathbf{u}_1|$, $D=4.9632$ eV is the energy of the valent coupling, and $\rho_0=1.418$ Å is the static length of valent bond;

$$U(\mathbf{u}_1,\mathbf{u}_2,\mathbf{u}_3) = \epsilon_v(\cos\varphi-\cos\varphi_0)^2, \tag{27}$$

where

$$\cos\varphi = (\mathbf{u}_3-\mathbf{u}_2,\mathbf{u}_1-\mathbf{u}_2)(|\mathbf{u}_3-\mathbf{u}_2|\cdot|\mathbf{u}_2-\mathbf{u}_1|)^{-1},$$

and $\cos\phi_0=\cos(2\pi/3)=-1/2$. Finally,

$$W(\mathbf{u}_1,\mathbf{u}_2,\mathbf{u}_3,\mathbf{u}_4) = \epsilon_t[1-(\mathbf{v}_1,\mathbf{v}_2)(|\mathbf{v}_1|\cdot|\mathbf{v}_2|)^{-1}], \tag{28}$$

where $\mathbf{v}_1=(\mathbf{u}_2-\mathbf{u}_1)\times(\mathbf{u}_3-\mathbf{u}_2)$ and $\mathbf{v}_2=(\mathbf{u}_3-\mathbf{u}_2)\times(\mathbf{u}_4-\mathbf{u}_3)$. The model parameters such as $\alpha=1.7889$ Å^{-1}, $\epsilon_v=1.3143$ eV, and $\epsilon_t=0.499$ eV are obtained from the phonon frequency spectrum of a planar lattice of carbon atoms [7,8].

Equilibrium structure of the nanotube with index (m,m) can be characterized by three parameters: its radius R, the angle shift φ, and the longitudinal step h. Equilibrium positions of the atoms in the tube are given by the coordinates

$$x^0_{n,l,0} = h(n-1), \quad x^0_{n,l,1} = h(n-1),$$

$$y^0_{n,l,0} = R\cos(\phi_{n,l}), \quad y^0_{n,l,1} = R\cos(\phi_{n,l}+\varphi),$$

$$z^0_{n,l,0} = R\sin(\phi_{n,l}), \quad z^0_{n,l,1} = R\sin(\phi_{n,l}+\varphi), \tag{29}$$

with cylindrical angles $\phi_{n,l}=[l-1+(n-1)/2]\Delta\phi$ and the angular distance $\Delta\phi=2\pi/m$. In order to find the parameters R, φ, and h, we need to solve the minimization problem

$$P(\mathbf{u}^0_{n-1,l,1},\mathbf{u}^0_{n-1,l+1,0},\mathbf{u}^0_{n,l,0},\mathbf{u}^0_{n,l,1},\mathbf{u}_{n+1,l-1,1},\mathbf{u}^0_{n+1,l,0}) \to \min_{R,\varphi,h},$$

where we have introduced the notations $\mathbf{u}^0_{n,l,i}=(x^0_{n,l,i},y^0_{n,l,i},z^0_{n,l,i})$ and $i=0,1$. The resulting value of the energy is then used as the minimum value. For a nanotube of the (6,6) type, we find a radius $R=4.1782$ Å and a longitudinal step $h=1.2590$ Å, while for a nanotube of the (12,12) type, one obtains $R=8.3230$ Å and $h=1.2560$ Å.

If one wishes to study small-amplitude vibrations, it is more convenient to switch to local cylindrical coordinates $u_{n,l,k}$, $v_{n,l,k}$, $w_{n,l,k}$ defined by

$$x_{n,l,k} = x^0_{n,l,k} + u_{n,l,k},$$

$$y_{n,l,k} = y^0_{n,l,k} - v_{n,l,k}\sin\phi^0_{n,l,k} + w_{n,l,k}\cos\phi^0_{n,l,k},$$

$$z_{n,l,k} = z^0_{n,l,k} + v_{n,l,k}\cos\phi^0_{n,l,k} + w_{n,l,k}\sin\phi^0_{n,l,k}, \tag{30}$$

with the angle $\phi_{n,l,0}=[l-1+(n-1)/2]\Delta\phi$ and $\phi_{n,l,1}=\phi_{n,l,0}+\varphi$. In this coordinate system, the Hamiltonian of the carbon nanotube takes the form

$$\mathcal{H} = \sum_n\sum_{l=1}^{m}\left\{\tfrac{1}{2}M(\dot{\mathbf{x}}_{n,l},\dot{\mathbf{x}}_{n,l}) + P(\mathbf{x}_{n-1,l};\mathbf{x}_{n-1,l+1};\mathbf{x}_{n,l};\mathbf{x}_{n+1,l-1};\mathbf{x}_{n+1,l})\right\}, \tag{31}$$

where the six-dimensional vector $\mathbf{x}_{n,l}=(u_{n,l,0},v_{n,l,0},w_{n,l,0},u_{n,l,1},v_{n,l,1},w_{n,l,1})$ describes in local coordinates the shifting of the atoms located in the cell n,l from their equilibrium position.

The equations of motion for the Hamiltonian (31) are given by

$$\begin{aligned}-M\ddot{\mathbf{x}}_{n,l} &= -\mathbf{F}_{n,l}\\ &= P_{\mathbf{x}_1}(\mathbf{x}_{n,l};\mathbf{x}_{n,l+1};\mathbf{x}_{n+1,l};\mathbf{x}_{n+2,l-1};\mathbf{x}_{n+2,l})\\ &\quad + P_{\mathbf{x}_2}(\mathbf{x}_{n,l-1};\mathbf{x}_{n,l};\mathbf{x}_{n+1,l-1};\mathbf{x}_{n+2,l-2};\mathbf{x}_{n+2,l-1})\\ &\quad + P_{\mathbf{x}_3}(\mathbf{x}_{n-1,l};\mathbf{x}_{n-1,l+1};\mathbf{x}_{n,l};\mathbf{x}_{n+1,l-1};\mathbf{x}_{n+1,l})\\ &\quad + P_{\mathbf{x}_4}(\mathbf{x}_{n-2,l+1};\mathbf{x}_{n-2,l+2};\mathbf{x}_{n-1,l+1};\mathbf{x}_{n,l};\mathbf{x}_{n,l+1})\\ &\quad + P_{\mathbf{x}_5}(\mathbf{x}_{n-2,l};\mathbf{x}_{n-2,l+1};\mathbf{x}_{n-1,l};\mathbf{x}_{n,l-1};\mathbf{x}_{n,l}),\end{aligned} \tag{32}$$

with the function $P_{\mathbf{x}_i}=\frac{\partial}{\partial\mathbf{x}_i}P(\mathbf{x}_1,\mathbf{x}_2,\mathbf{x}_3,\mathbf{x}_4,\mathbf{x}_5)$, $i=1,2,\ldots,5$. In the linear approximation, the previous set of equations takes the form

$$\begin{aligned}-M\ddot{\mathbf{x}}_{n,l} &= B_1\mathbf{x}_{n,l} + B_2\mathbf{x}_{n+1,l} + B_2^*\mathbf{x}_{n-1,l} + B_3\mathbf{x}_{n+2,l} + B_3^*\mathbf{x}_{n-2,l}\\ &\quad + B_4\mathbf{x}_{n,l+1} + B_4^*\mathbf{x}_{n,l-1} + B_5\mathbf{x}_{n+1,l-1} + B_5^*\mathbf{x}_{n-1,l+1}\\ &\quad + B_6\mathbf{x}_{n+2,l-1} + B_6^*\mathbf{x}_{n-2,l+1} + B_7\mathbf{x}_{n+2,l-2} + B_7^*\mathbf{x}_{n-2,l+2},\end{aligned} \tag{33}$$

where the matrix coefficients are defined as

$$B_1 = P_{\mathbf{x}_1\mathbf{x}_1} + P_{\mathbf{x}_2\mathbf{x}_2} + P_{\mathbf{x}_3\mathbf{x}_3} + P_{\mathbf{x}_4\mathbf{x}_4} + P_{\mathbf{x}_5\mathbf{x}_5},$$

$$B_2 = P_{\mathbf{x}_1\mathbf{x}_3} + P_{\mathbf{x}_3\mathbf{x}_5}, \quad B_3 = P_{\mathbf{x}_1\mathbf{x}_5},$$

$$B_4 = P_{\mathbf{x}_1\mathbf{x}_2} + P_{\mathbf{x}_4\mathbf{x}_5}, \quad B_5 = P_{\mathbf{x}_2\mathbf{x}_3} + P_{\mathbf{x}_3\mathbf{x}_4},$$

$$B_6 = P_{\mathbf{x}_1\mathbf{x}_4} + P_{\mathbf{x}_2\mathbf{x}_5}, \quad B_7 = P_{\mathbf{x}_2\mathbf{x}_4},$$

with the matrix of partial derivatives

$$P_{\mathbf{x}_i,\mathbf{x}j} = \frac{\partial^2 P}{\partial\mathbf{x}_i\partial\mathbf{x}_j}(\mathbf{0},\mathbf{0},\mathbf{0},\mathbf{0},\mathbf{0}), \quad i,j=1,2,3,4,5.$$

The solution of the linearized equations (33) can be found in terms of plane waves in the form

$$\mathbf{x}_{nl} = A\mathbf{e}\exp(iqn + il\delta\phi - i\omega t), \tag{34}$$

where A stands for the amplitude of the wave, $\mathbf{e}$ is the unit vector of the amplitude, $q\in[0,\pi]$ is the dimensionless wave number, and $\delta=2\pi j/m$ $(j=0,1,\ldots,m-1)$ is the dimension-

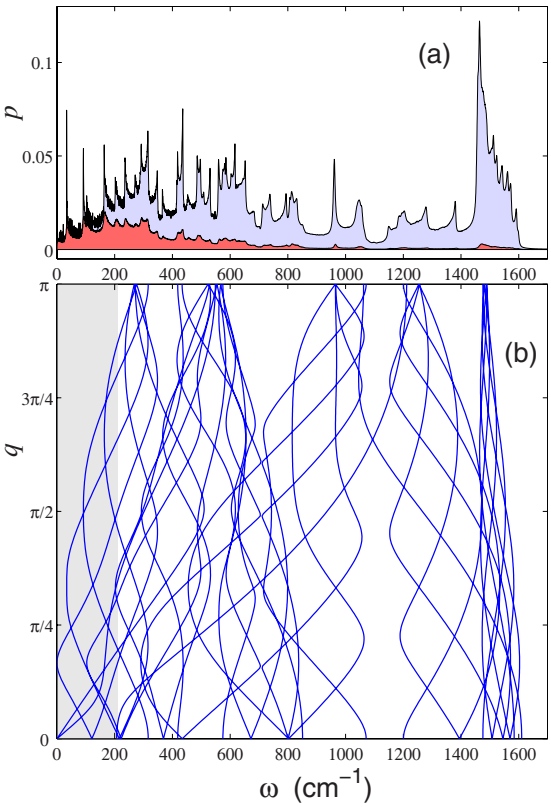

FIG. 5. (Color online) (a) Spectral density of thermal oscillations of armchair (6, 6) carbon nanotube for $T=300$ K (red field corresponds to system equations with color noise) and (b) 60 dispersion curves of the phonon modes. Gray marks the frequency region $\omega < k_B T/\hbar$.

less orbital moment of the phonon. By injecting the expression (34) into the linear equation system (33), we obtain the eigenvalue problem

$$M\omega^2\mathbf{A} = [B_1 + B_2 e^{iq} + B_2^* e^{-iq} + B_3 e^{2iq} + B_3^* e^{-2iq} + B_4 e^{i\delta} + B_4^* e^{-i\delta} + B_5 e^{iq-i\delta} + B_5^* e^{-iq+i\delta} + B_6 e^{2iq-i\delta} + B_6^* e^{-2iq+i\delta} + B_7 e^{2iq-2i\delta} + B_7^* e^{-2iq+2i\delta}]A. \quad (35)$$

Thus, the calculation of the dispersion curves of the carbon nanotube requires the computation of the eigenvalues of the Hermitian matrix of dimension 6×6 (35) at each value of the wave number $0 \leqslant q \leqslant \pi$ and the moment $\delta = 2\pi j/m$ ($j=0,1,\ldots,m-1$). The dispersion curves obtained in this way consists of $6m$ branches [see Fig. 5(b)].

The computation of the eigenvalues (35) yields not only all the dispersion curves $\omega(q)$ but also the spectral density $p(\omega)$, normalized according to $\int_0^\infty p(\omega)d\omega = 1$.

A simple method for obtaining the temperature dependence of the spectral density consists in making a simulation of the thermal vibrations of the carbon nanotube. To this aim, the system is first driven to thermal equilibrium using the usual Langevin equations with white noise

$$M\ddot{\mathbf{x}}_{n,l} = \mathbf{F}_{n,l} - \Gamma M\dot{\mathbf{x}}_{n,l} + \Xi_{n,l}, \quad (36)$$

with the dissipation coefficient $\Gamma = 1/t_r$, t_r is the relaxation time of atoms (it is reasonable to take $t_r = 0.1$ ps), and $\Xi_{n,l} = (\xi_{n,l,1}, \ldots, \xi_{n,l,6})$ is the six-dimensional vector corresponding to the normally distributed random noises, describing the interaction of the particles located in the cell (n,l) with the thermal bath. The characteristic correlation functions of these noises can be written as

$$\langle \xi_{n,k,i}(t_1)\xi_{m,l,j}(t_2)\rangle = 2Mk_B T\delta_{nm}\delta_{kl}\delta_{ij}\delta(t_1 - t_2), \quad (37)$$

where k_B is the Boltzmann constant and T is the temperature of the thermostat. After having set the initial coordinates (29) and velocities to zero, the numerical integration of the system of Langevin equations was performed over $t = 20t_r$.

Once the system evolves into thermal equilibrium, we used the thermalized states $\{\mathbf{x}_{n,l}, \dot{\mathbf{x}}_{n,l}\}$ obtained in this way as initial conditions for the evolution of the isolated system defined by the equations of motion

$$M\ddot{\mathbf{x}}_{n,l} = \mathbf{F}_{n,l}.$$

The numerical integration of this set of equations yields the time dependence of the particle velocity $\dot{\mathbf{x}}_{n,l}(t)$. By Fourier-transforming this particle velocity (for numerical evaluations, it is convenient to use fast Fourier transformation), one finally obtains the spectral density of vibrations $p(\omega)$ of the particles in the system. In order to increase the accuracy of the result, the spectral density was obtained from 100 independent thermalization processes and averaged over the atoms of the system.

The spectral density profile obtained at $T = 300$ K is shown in Fig. 5(a). We notice that at this temperature, the density profile is in good agreement with the shape of the dispersion curves, which can be seen as a weak manifestation of nonlinearity effects. If one assumes that the proper vibrational modes of the carbon nanotube remain linear, then the specific heat of the nanotube can be deduced from the integral

$$c(T) = \int_0^{+\infty} c_q(\omega)p(\omega)d\omega,$$

$$c_q(\omega) = \left(\frac{\hbar\omega}{k_B T}\right)^2 \frac{\exp(\hbar\omega/k_B T)}{[\exp(\hbar\omega/k_B T) - 1]^2}, \quad (38)$$

where $c_q(\omega)$ is the dimensionless thermal capacity of phonons with angular frequency ω. This computation method based on the spectral density summation was first used to compute the heat capacity of carbon nanotubes in Refs. [9,10].

This approach is remarkably practical since the specific heat of the system follows from the simple knowledge of the spectral density $p(\omega)$ of thermal vibrations. On the other hand, the spectral density can be deduced from the shape of the spectral curves, that is, by considering the latter as the frequency spectrum of the harmonic modes in the nanotube. The heat capacity $c(T)$ of the carbon nanotube with index (6,6), (12,12), and (10,0) obtained in this way is shown in Fig. 6. It is clearly seen in this figure that the specific heat is practically insensitive to the index of the nanotube. Furthermore, the temperature dependence of the specific heat is linear in the regime $0 < T < 400$ K. This temperature behavior of the specific heat is in concordance with previous theoret-

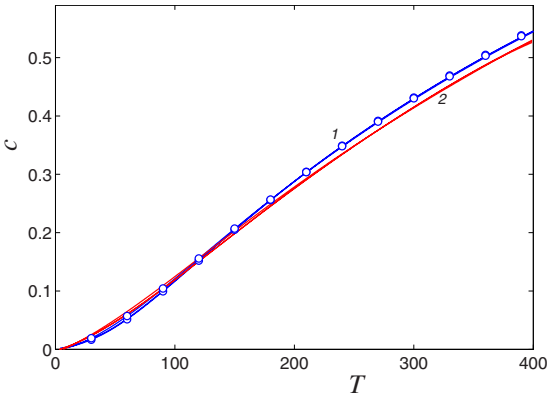

FIG. 6. (Color online) Temperature dependence of specific heat c of carbon nanotube (6,6), (12,12), and (10,0). Blue line (curve 1) corresponds to the result obtained with the use of the frequency density of linear phonon waves while markers were obtained from the frequency density of thermal vibrations. Red line (curve 2) corresponds to the result obtained from the numerical integration of Langevin equations with color noise.

ical works [9,10] and confirms the experimental measures of the specific heat of titanium dioxide nanotubes [11].

We can equally obtain the spectral density that appears in Eq. (38) directly from dynamical simulations, i.e., by following thermal vibrations of atoms in the carbon nanotube at finite temperature $T>0$. As it can be checked in Fig. 6, numerical simulations show that these two approaches yield almost the same result (the spectral density has a weak temperature dependence).

Let us note that the numerical integration of the Langevin equations with white noise (36) that allows us to obtain the dimensionless specific heat of the nanotube $(m,0)$ from the equation $c(T)=(d\langle H\rangle/dT)/(6Nmk_B)$, where Nh is the length of the nanotube, shows that the heat capacity is practically independent of the temperature, that is, $c=1$ over $0<T<400$ K (this behavior follows from the well-known equipartition theorem of classical statistical mechanics, which states that the mean energy of each degree of freedom is equal to k_BT). But the situation drastically changes if one replaces the white noise of the Langevin equation with a time-correlated color noise whose temperature dependence is given by the formula (11). In this case, thermal vibrations of the nanotube are described by the system of Langevin equations,

$$M\ddot{\mathbf{x}}_{n,l} = \mathbf{F}_{n,l} - \Gamma M\dot{\mathbf{x}}_{n,l} + \Xi_{n,l}, \tag{39}$$

$$\dot{\Xi}_{n,l} = (\Theta_{n,l} - \Xi_{n,l})/t_c, \tag{40}$$

where $\Theta_{n,l}=(\eta_{n,l,1},\ldots,\eta_{n,l,6})$ is the six-dimensional vector corresponding to the normally distributed random noise and normalized according to Eq. (37), the relaxation time $t_r=1$ ps, and the correlation time of random noises $t_c=\hbar\sqrt{e-2}/k_BT$.

The numerical integration of the equations of motion (39) and (40) first yields the mean energy of the nanotube $E=\langle H\rangle$ versus temperature T. Then the specific heat is deduced from the relation $c(T)=dE/dT$. The result is illustrated in Fig. 6. First of all, it is clearly seen that the specific heat of nanotubes (6,6), (12,12), and (10,0) has practically the same temperature behavior, that is, it tends to zero for $T\to 0$ and it rises regularly with the increase of the temperature. Furthermore, the specific heat calculated with color noise coincides very well with the one obtained from Eq. (38) via computation of the spectral density.

We show in Fig. 5(a) the shape of the spectral density of thermal vibrations of the carbon nanotube, obtained with color noise. We can note that only low-frequency vibrations characterized by $\omega<k_BT/\hbar$ are totally thermalized while the thermalization of high-frequency modes is partial. Moreover, the degree of thermalization decreases with increasing temperature.

IV. COMPUTATION OF THE HEAT CAPACITY OF POLYETHYLENE MACROMOLECULES

By considering the concrete example of carbon nanotubes, we have shown that the use of the Langevin equations with color noise (39) and (40) allows us to realize the quantum effect of partial thermalization of high-frequency modes and yields the correct temperature behavior of the specific heat for complex molecular systems. The proposed method becomes very useful, especially for molecular systems with complex configurational dynamics, for example in the case of macromolecules that possess globular structure, or simply when one deals with a highly nonlinear dynamics and it becomes meaningless to consider the existence of a spectral density of linear small-amplitude vibrations.

Let us prove the efficiency of the method by considering a further example, that is, the polyethylene macromolecule $(CH_2)_{1000}$. We will use a united atom model where the hydrogen atoms are lumped onto the carbon atoms to which they are attached.

Let the vector $\mathbf{u}_n=(x_n,y_n,z_n)$ be the coordinate of the nth carbon atom of the polyethylene molecule (PE) and $n=1,2,\ldots,N$, where N is the total number of carbon atoms. Thus the Hamiltonian of the macromolecule takes the form

$$H = \sum_{n=1}^{N}\frac{1}{2}M(\dot{\mathbf{u}}_n,\dot{\mathbf{u}}_n) + \sum_{n=1}^{N-1}V(\mathbf{u}_n,\mathbf{u}_{n+1}) + \sum_{n=1}^{N-2}U(\mathbf{u}_n,\mathbf{u}_{n+1},\mathbf{u}_{n+2}) + \sum_{n=1}^{N-3}W(\mathbf{u}_n,\mathbf{u}_{n+1},\mathbf{u}_{n+2},\mathbf{u}_{n+3}) + \sum_{n=1}^{N-4}\sum_{k=n+4}^{N}P(\mathbf{u}_n,\mathbf{u}_k). \tag{41}$$

The first summation in this expression corresponds to the kinetic energy of the macromolecule, and $M=14m_p$ is the mass of the atom groups CH_2, where $m_p=1.6603\times10^{-27}$ kg is the mass of a proton. The second term gives the deformation energy of covalent bonds, the third term is the energetic cost corresponding to the change of covalent angles, the forth term is the energy for the variation of torsional angles, and the final term is the energy of Van der Waals interactions.

Following the work [14], let us model the covalent bonds CH_2-CH_2 with the potential

$$V(\mathbf{u}_n,\mathbf{u}_{n+1}) = \frac{1}{2}K(r_n - r_0)^2, \tag{42}$$

where $r_n=|\mathbf{u}_{n+1}-\mathbf{u}_n|$ is the length of the nth covalent bond, $r_0=1.53$ Å is the equilibrium length of covalent bonds, and $K=700$ kcal/mol Å^{-2} is the stiffness of the links. The potential of the covalent angle CH_2-CH_2-CH_2 is given by

$$U(\mathbf{u}_n,\mathbf{u}_{n+1},\mathbf{u}_{n+2}) = \epsilon_\theta(\cos\theta_n - \cos\theta_0)^2, \tag{43}$$

where the cosine function for the angle of the nth covalent angle

$$\cos(\theta_n) = (\mathbf{u}_{n+1}-\mathbf{u}_n,\mathbf{u}_{n+2}-\mathbf{u}_{n+1})/r_n r_{n+1},$$

the equilibrium value of the angle $\theta_0=109°$, and the energy $\epsilon_\theta=67.114$ kcal/mol. The potential energy of the torsional angle can be expressed as

$$W(\mathbf{u}_n,\mathbf{u}_{n+1},\mathbf{u}_{n+2},\mathbf{u}_{n+3}) = \epsilon_0 - \epsilon_1\cos(\phi_n) - \epsilon_2\cos(2\phi_n) - \epsilon_3\cos(3\phi_n), \tag{44}$$

where the characteristic energies are $\epsilon_1=0.81$ kcal/mol, $\epsilon_2=-0.43$ kcal/mol, $\epsilon_3=1.62$ kcal/mol, $\epsilon_0=\epsilon_1+\epsilon_2+\epsilon_3$, and finally ϕ_n is the angle between the vectors $(\mathbf{u}_{n+1}-\mathbf{u}_n)\times(\mathbf{u}_{n+2}-\mathbf{u}_{n+1})$ and $(\mathbf{u}_{n+2}-\mathbf{u}_{n+1})\times(\mathbf{u}_{n+3}-\mathbf{u}_{n+2})$. The Van der Waals potential is given by

$$P(\mathbf{u}_n,\mathbf{u}_k) = 4\epsilon_{LJ}[(\sigma/r_{nk})^{12} - (\sigma/r_{nk})^6], \tag{45}$$

where $r_{nk}=|\mathbf{u}_k-\mathbf{u}_n|$ is the distance between the nth and kth carbon atoms, the interaction energy $\epsilon_{LJ}=0.112$ kcal/mol, and $\sigma=4.01$ Å. In order to reduce the computational time, we truncate the Van der Waals potential at the distance 100 Å. These potentials were parametrized using experimental data and quantum calculations on short alkanes and have been shown to provide an accurate description of polyethylene melts [14–16].

Thermal fluctuations of the macromolecule can be described within the framework of the classical mechanics by using Langevin equations with white noise,

$$M\ddot{\mathbf{u}}_n = -\frac{\partial H}{\partial \mathbf{u}_n} - \Gamma M\dot{\mathbf{u}}_n + \Theta_n,$$

$$n = 1,2,\ldots,N, \tag{46}$$

with the dissipation coefficient $\Gamma=1/t_r$, and $\Theta_n=(\theta_{n,1},\theta_{n,2},\theta_{n,3})$ is the three-dimensional vector corresponding to the normally distributed random noises, describing the interaction of the nth carbon atom with the thermal bath. The characteristic correlation functions of these noises are given by

$$\langle\theta_{n,i}(t_1)\theta_{k,j}(t_2)\rangle = 2Mk_BT\delta_{nk}\delta_{ij}\delta(t_1-t_2). \tag{47}$$

The planar transzigzag conformation of the polyethylene macromolecule

$$u_{n,l} = nl_x, \quad u_{n,2} = (-1)^n l_y/2, \quad u_{n,3} = 0,$$

$$\dot{u}_{n,i} = 0, \quad n = 1,2,\ldots,N, \quad i = 1,2,3 \tag{48}$$

was chosen as initial conditions, where $l_x=r_0\sin(\theta_0/2)$ and $l_y=r_0\cos(\theta_0/2)$ are longitudinal and transversal steps of the transzigzag chain. We should note that the transzigzag configuration (48) will be the ground state of the macromolecule only if we fix its ends, that is, if we impose $\dot{\mathbf{u}}_1\equiv 0$, $\dot{\mathbf{u}}_N\equiv 0$. In this case, the macromolecule will always keep its linear transzigzag form. On the other hand, the macromolecule with free ends will return to its ball configuration since this state is energetically more favorable in the sense that it allows the molecule to form more nonvalent interatomic bonds.

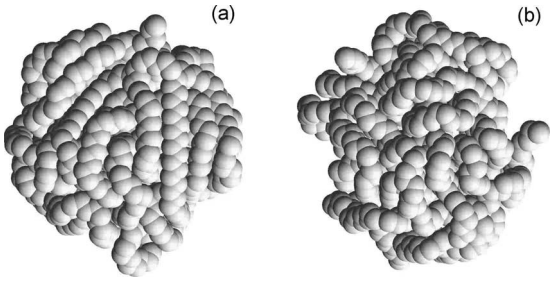

FIG. 7. Ball conformation of a single chain $(CH_2)_{1000}$ for (a) temperature $T=0$ and (b) $T=300$ K.

The numerical integration of the equations of motion (46) with initial conditions (48) showed that for $t_r=1$ ps and at temperature $T=300$ K, the macromolecule PE which consists of $N=1000$ units returns to its ball configuration in 2 ns—see Fig. 7(b). By further integrating the equations of motion at absolute zero temperature $T=0$, one obtains the ground-state ball conformation of the macromolecule—see Fig. 7(a). It is clearly seen that at room temperature $T=300$ K, the globular shape of the PE macromolecule becomes more irregular.

In order to find the spectral density of thermal fluctuations of the macromolecule by using Langevin equations (46), we first obtain the initial conditions of the system corresponding to the thermalized state of the macromolecule. This is done by numerically integrating the equations of motion over $t=20t_r$. In the case of the boundary conditions with fixed ends, we should use the initial conditions (47) corresponding to the plane transzigzag configuration, and if one instead considers free boundary conditions, one should use as initial conditions the ball configuration of the macromolecule. The next step consists in decoupling the thermalized chain from the bath and calculating the spectral density $p(\omega)$ of the kinetic energy distribution of the carbon atoms by following the real-time dynamics of the isolated system. In order to increase the accuracy of the result, the spectral density was obtained from 200 independent thermalization processes and averaged over all atoms of the chain.

The spectral density profile of linear transzigzag and ball conformations of the single PE macromolecule is shown in Fig. 8. One can notice that the frequency spectrum of the transzigzag configuration consists of two zones. The first low-frequency regime defined by $0\leqslant\omega\leqslant 473$ cm^{-1} corresponds to the planar acoustic fluctuations and nonplanar torsional vibrations of the zigzag structure. The second zone which covers the high-frequency regime $1037\leqslant\omega\leqslant 1251$ cm^{-1} corresponds to the planar optical vibrations of the zigzag. A detailed description of linear vibrations of the zigzag structure was given in Refs. [17–20]. By inspecting Fig. 8(a), one can notice that at $T=1$ K, thermal fluctuations

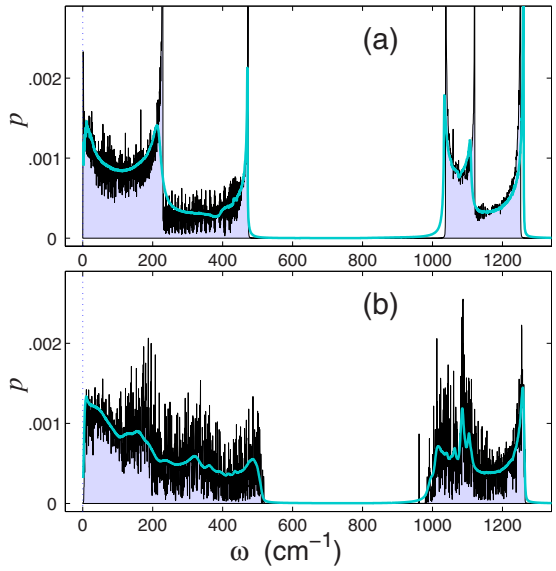

FIG. 8. (Color online) Spectral density of thermal vibrations of the (a) transzigzag and (b) ball conformation of the single polyethylene macromolecule $(CH_2)_{1000}$. The thin curve on the top of the gray region gives the density at low temperature, $T=1$ K, and the bold curve gives the density at room temperature, $T=300$ K.

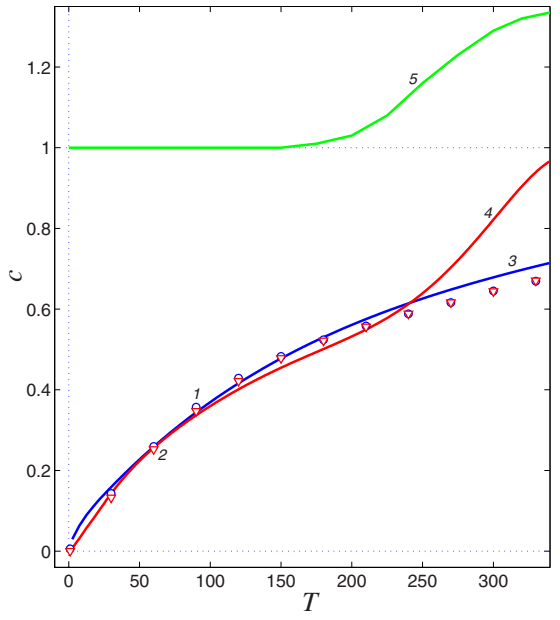

FIG. 9. (Color online) Temperature dependence of the dimensionless specific heat c of the macromolecule $(CH_2)_{1000}$. Markers 1 and 2 correspond to the heat capacity of transzigzag and ball conformations of the macromolecule, respectively. These results were obtained with the use of the frequency density of thermal vibrations. Blue line 3 and red line 4 correspond to the heat capacity of transzigzag and ball conformations. These results were obtained with the use of Langevin equations with color noise. Green curve 5 corresponds to the heat capacity of the ball conformation. This result was obtained from classical Langevin equations with white noise.

of the transzigzag with fixed ends are mainly linear and the density of the frequency spectrum indicates a marked singular behavior at the boundary of the zone corresponding to linear vibrations. With the increase of the temperature from 0 to 300 K, a weak change of the spectral density, that is, an insignificant broadening of the optical zone, takes place. The spectral density of thermal fluctuations of the ball configuration PE is illustrated in Fig. 8(b). The spectral density is once again composed of two zones, a low-frequency acoustic zone $0 \leqslant \omega \leqslant 518$ cm^{-1} and a high-frequency optical zone $962 \leqslant \omega \leqslant 1266$ cm^{-1}. The more pronounced width of these zones is due to the irregularity of the ball configuration. This figure undoubtedly shows that the spectral density is practically insensitive to the increase of the temperature from 1 to 300 K.

With the knowledge of the spectral density of thermal fluctuations $p(\omega)$ and using Eq. (38), we are now able to calculate the temperature dependence of the dimensionless specific heat. Let us recall that the formula (38) remains valid only if one deals with linear vibrations of the molecular system. The heat capacity $c(T)$ of the PE macromolecule obtained in this way is shown in Fig. 9 (markers 1 and 2). These two plots show that within the physically acceptable interval $30 \leqslant T \leqslant 340$ K, the computational method yields almost the same trend for the specific heat of the ball and zigzag configurations.

We will now show that the situation changes significantly if one computes the specific heat $c(T)$ by using Langevin equations with color noise,

$$M\ddot{\mathbf{u}}_n = -\frac{\partial H}{\partial \mathbf{u}_n} - \Gamma M\dot{\mathbf{u}}_n + \Xi_n, \tag{49}$$

$$\dot{\Xi}_n = (\Theta_n - \Xi_n)/t_c, \tag{50}$$

where Θ_n is the three-dimensional vector corresponding to the normally distributed random noise satisfying the correlation functions (47), the relaxation time $t_r=1$ ps, and the correlation time of random noises, $t_c=\hbar\sqrt{e-2}/k_BT$. The numerical integration of the Langevin equations with color noise (49) and (50) allows us to obtain the dimensionless specific heat of the PE macromolecule from the equation

$$c(T) = \frac{1}{3Nk_B}\frac{d\langle H\rangle}{dT},$$

where $N=1000$ is the total number of carbon atoms in the macromolecule.

By inspecting the curve 3 and the markers 1 of Fig. 9, one can observe that the specific heat of the linear macromolecule with fixed ends (transzigzag conformation) calculated with generalized Langevin equations (49) and (50) agrees very well with the result obtained from the spectral density formula (38). One thus recovers here the same concordance between both methods as in the case of the carbon-nanotube example. We should also note that in the considered temperature regime, the nonlinearity of the Hamiltonian has a weak contribution and the dynamics is essentially linear. This aspect explains the good agreement between the proposed

method and the spectral density formula and the validity of the latter for the calculation of the specific heat.

If one now considers the macromolecule with free ends (ball conformation), both computational methods still yield a similar result for temperatures $T<210$ K. On the other hand, a significant discrepancy between these approaches takes place for $T>210$ K—see Fig. 9, marker 2 and curve 4. The disagreement results from a quite fast increase of the specific heat, computed using Langevin equations with color noise, with the increase of the temperature above this threshold.

To understand this effect, let us consider the temperature dependence of the specific heat within the framework of classical mechanics. One should use in this case Langevin equation with white noise (46). At low temperatures, the specific heat of the ball is practically constant, that is, $c=1$ for $0\leqslant T<200$ K, while for $T>200$ K, the specific heat rises steadily—see Fig. 9, curve 5. This sharp increase is indeed due to the melting phase transition of the ball structure. The ball conformation remains stable due to weak Wan del Waals interactions, whose strength sharply decreases with increasing temperature. For $T<200$ K, the ball possesses a compact and regular structure [see Fig. 7(a)], while at $T>200$ K it becomes more mobile and irregular [see Fig. 7(b)]. In other words, at low temperatures the ball conformation is frozen, and at high temperatures it behaves as a liquid. The sharp increase of the specific heat is thus related with the transition of the ball structure from solid to liquid state.

We have seen that the dynamics of the ball is highly nonlinear for $T>200$ K and the approach that consists in computing the heat capacity thorough the spectral density consequently fails. This method is clearly not able to distinguish the transition point of the ball structure, and the failure can be qualitatively understood by noticing that the frequency spectrum is practically unchanged at the transition—see Fig. 8(b). On the other hand, the proposed method of generalized Langevin equations keeps working even above the critical point ($T>200$ K) since it is able to reproduce the sharp increase of the specific heat which accompanies the melting phase transition of the ball structure—see Fig. 9, curves 4 and 5. Hence the generalized Langevin equation method seems to be the most adequate approach if one wishes to calculate the specific heat of the ball macromolecule PE in the high-temperature regime $T>200$ K.

Let us note that the case that we have considered above concerns the majority of protein macromolecules. At room temperature, these molecules manifest globular form with a high mobility, which is a necessary condition for their biological functions. The importance of the proposed method for practical applications in biophysics is thus clear.

It is of course imperative to identify the limitations of the proposed method. The generalized Langevin equation approach is clearly not an exact method and simply aims at providing an analogous modeling of the quantum partial thermalization effect. Figures 1–3 provide some quantitative insight about the limit of the generalized Langevin approach. By comparing the plots of these figures, we notice that in the presence of an intersite nonlinearity, the statistical method and the Langevin method yield a reasonable agreement over the whole temperature regime, see Fig. 2 and the top plot of Fig. 3. On the other hand, in the presence of an on-site nonlinearity, the Langevin method slightly overestimates the specific heat in the high-temperature regime, while the agreement in the quantum regime $T<T_E$ survives.

A further weakness of the method is its inability to reproduce the ground-state fluctuations of molecular systems. But we should also note that the zero vibrations give significant contributions to the specific heat exclusively at very low temperatures, where it becomes meaningless to use the Langevin equations with color noise. In this temperature regime, it would be more reasonable to calculate the specific heat through the spectral density formula (38). As we have shown in the case of the carbon nanotube model and the polyethylene macromolecule, generalized Langevin equations remain valid in the temperature range 30–350 K.

Moreover, we would like to emphasize that in the case of the usual Langevin equations with white noise, the generalized equipartition theorem guarantees the convergence toward an equilibrium state at which one can unambiguously define a mean energy and specific heat. If one instead considers a correlated color noise, the equipartition theorem does not hold and the definition of an equilibrium state is more ambiguous. In this case, one can indeed obtain a thermal equilibrium configuration only if the color noise is applied to all components of the system with the same amplitude.

Finally, the use of Langevin equations with color noise may lead in specific situations to the directional motion of the system—the so-called ratchet dynamics. Some symmetry breaking is of course necessary for the apparition of the ratchet effect (see, for example, [12,13]). It is clear that isolated macromolecules cannot undergo a directional dynamics. The existence of this kind of dynamics for example, would, require the existence of an asymmetric substrate. On the other hand, even if there exists in the system some ratchet tendency, it would manifest itself in the long-time limit and give a very small contribution to the specific heat.

There already exists some quantum-mechanical algorithms to evaluate thermal equilibrium averages: to name but a few, the *path-integral Monte Carlo* approach and the *quantum Langevin equation* method. The former approach consists in discretizing space and time variables of the Euclidean action [21,22]. The d-dimensional quantum partition function is recast in this way into a $(d+1)$-dimensional classical partition function. When one deals with a nonlinear N-body system, the evaluation of the corresponding $(d+1)$-dimensional effective partition function is very complicated even in the case $d=1$ since the numerical transfer-matrix method can be applied exclusively to one-dimensional Hamiltonians. One thus has to run Monte Carlo simulations in order to calculate the $(d+1)$-dimensional effective partition function. It is clear in this case that the increase of the spatial dimension by 1 multiplies the simulation time by the Trotter number, which should be large enough to obtain a reliable result. On the other hand, the additional numerical cost of the generalized Langevin method compared to classical Langevin simulations is obviously irrelevant since the approximative consideration of the quantum mechanics in the proposed approach simply consists in introducing a single additional degree of freedom. A numerically tractable formulation of the quantum Langevin equation

method was recently proposed in Ref. [23] in the context of the heat conduction problem. The method consists in integrating the quantum Langevin equations over the bath degrees of freedom, which leads to reduced equations describing only the evolution of the subsystem. Since the oscillator chain is connected to the external heat baths only at its extremities, the numerical integration of the reduced Langevin equations becomes possible. If we instead assume that each oscillator is connected to the external reservoir, as required if one needs to compute thermal averages in the canonical ensemble, the numerical cost of the algorithm would be highly increased due to the matricial term corresponding to the integral of the memory function (self-energy matrix).

An absolute and precise comparison of the computational speed of the proposed method with the speed of other quantum algorithms is difficult, since this comparison will depend strongly on the considered model. It is, however, clear that in any case, the generalized Langevin method discussed in this work is much faster. The discussion of the numerical efficiency can be done by comparing the efficiency of classical molecular dynamics and quantum molecular dynamics. Quantum molecular dynamics is quite different from classical molecular dynamics, which is primarily concerned with the classical motion of atoms interacting according to a given potential. Quantum algorithms are based on the laws of quantum mechanics, the fundamental equations that describe electrons and phonons. The equations that should be solved in quantum calculations are extraordinary complex. Modeling the behavior of molecules at the quantum level requires unprecedented computational power and speed. The largest systems that can deal with the current computational power of massively parallel computers are Hamiltonian models composed of a few hundred atoms and thousands of electrons, while on the classical level, one can simulate the dynamics of Hamiltonian systems as large as 10^5 atoms.

V. CONCLUSIONS

We proposed a method for computing the temperature dependence of the heat capacity in complex molecular systems. The proposed scheme is based on the use of the Langevin equation with low-frequency color noise. We showed that the thermal behavior of the correlation time of random forces, which is the key characteristic of the partial thermalization effect, can be described by a linear function of the inverse bath temperature, that is, $t_c=\hbar\sqrt{e-2}/k_BT$. We next illustrated nonlinearity effects by considering two simple Hamiltonian models, and we explicitly showed that the generalized Langevin approach can be used in the presence of anharmonicities in the Hamiltonian. Then we used our approach to calculate the specific heat of one-dimensional ϕ^4 and FPU-β models. By comparing the result with the one obtained from the quantum self-consistent phonon method, we demonstrated the validity of the generalized Langevin approach for many-body systems. Finally, by applying the proposed procedure to carbon nanotubes and polyethylene macromolecules, we showed that the consideration of the color noise in the Langevin equation allows us to accurately reproduce the temperature evolution of the specific heat in high-dimensional complex systems.

It is well known that for complex systems having strong nonlinearity effects in the quantum regime ($T<T_E$), there exists a temperature gap unreachable by existing approximative approaches such as the spectral density equations (38), while the drawback of quantum Monte-Carlo–Langevin methods is the large numerical cost in the case of many particle models. The proposed method may be very useful to fill this gap, especially if one wishes to investigate the thermodynamics of realistic molecular systems with complex configurational dynamics, for example in the case of macromolecules that possess globular structures with a highly nonlinear dynamics. Further investigation is of course necessary to better understand the limitations of our method and also to fix its potential applications, especially for nonequilibrium issues such as the heat transport in complex lattice systems.

ACKNOWLEDGMENTS

Alexander Savin thanks the Hong Kong Baptist University for warm hospitality during his stay in Hong Kong. This work was supported in part by grants from the Hong Kong Research Grants Council and Hong Kong Baptist University.

APPENDIX A: THE SPECIFIC HEAT OF THE OSCILLATOR CHAINS FROM THE FIRST-ORDER VARIATIONAL APPROACH

In this appendix, we will give a brief presentation of the calculation of the heat capacities for one-dimensional FPU-β (14) and ϕ^4 (17) models by using the first-order self-consistent phonon theory (SCPT). A detailed description of the derivation of the first-order free energy within the path-integral approach will be given elsewhere [24].

In the path-integral representation of quantum-statistical mechanics, the N-body partition function in the canonical ensemble can be expressed as a path integral over close trajectories,

$$Z=\int D\mathbf{x}e^{-S[\mathbf{x}]}, \tag{A1}$$

where

$$S=\int_0^{\hbar\beta}d\tau\left(\frac{m}{2}\dot{\mathbf{x}}^2+U[\mathbf{x}]\right) \tag{A2}$$

is the Euclidean action. The idea of the SCPT thus consists in approximating the original Euclidean action (A2) with a quadratic trial action that allows an exact evaluation of the trace (A1). The trial action is chosen in the form

$$S_0=\int_0^{\beta\hbar}d\tau H_0 \tag{A3}$$

with

$$H_0=\sum_{k=1}^{N}\left\{\frac{m}{2}\dot{x}_k^2+\frac{\lambda_1}{2}x_k^2+\lambda_2x_k+gx_kx_{k-1}\right\}. \tag{A4}$$

The parameters of the trial Hamiltonian (A4) are to be fixed by minimizing the first-order free energy according to the Feynman-Jensen inequality,

$$F \leqslant F_0 + \langle H - H_0 \rangle. \tag{A5}$$

The minimized free energy per particle of the FPU-β model takes the form

$$f_1 = f_0 - \frac{3\lambda}{4}\langle \delta x_i^2 \rangle^2 \tag{A6}$$

with

$$f_0 = -\frac{k_B T}{N} \ln Z_0,$$

$$Z_0 = \prod_{p=1}^{N} \frac{\sin(p\pi/N)}{\sinh(\beta\hbar\sigma_p/2)}, \tag{A7}$$

and the pseudophonon frequencies and the lattice displacement are self-consistently calculated by solving the corresponding equations,

$$\langle \delta x^2 \rangle = \frac{\hbar}{2Nm} \sum_p \frac{4 \sin^2\left(\frac{p\pi}{N}\right)}{\sigma_p} \coth\left(\frac{\beta\hbar\sigma_p}{2}\right),$$

$$m\sigma_p^2 = f_0 + 4(K + 3\lambda\langle \delta x^2 \rangle)\sin^2\left(\frac{p\pi}{N}\right). \tag{A8}$$

The first-order free energy for ϕ^4 model can be expressed as

$$f_1 = f_0 - \frac{3\lambda}{4}\langle x_i^2 \rangle^2, \tag{A9}$$

where

$$f_0 = -\frac{k_B T}{N} \ln Z_0,$$

$$Z_0 = \prod_{p=1}^{N} \frac{1}{\sinh(\hbar\beta\sigma_p/2)}, \tag{A10}$$

and the self-consistent equations to be solved by iteration read

$$\langle x^2 \rangle = \frac{\hbar}{2Nm} \sum_p \sigma_p^{-1} \coth\left(\frac{\beta\hbar\sigma_p}{2}\right),$$

$$m\sigma_p^2 = f_o + 3\lambda\langle x^2 \rangle + 4K \sin^2\left(\frac{\pi p}{N}\right). \tag{A11}$$

The specific heats follow from Eqs. (A6) and (A9) according to Eq. (16).

[1] A. Einstein, Ann. Phys. **22**, 180 (1907).
[2] C. W. Gardier, *Handbook of Stochastic Methods*, 2nd ed. (Springer, Berlin, 1985).
[3] N. G. van Kampen, *Stochastic Processes in Physics and Chemistry* (Elsevier, Amsterdam, 1992).
[4] D. W. Noid *et al.*, Macromolecules **24**, 4148 (1991).
[5] B. G. Sumpter *et al.*, Adv. Polym. Sci. **116**, 27 (1994).
[6] A. V. Savin and L. I. Manevitch, Phys. Rev. B **58**, 11386 (1998); **67**, 144302 (2003).
[7] R. Al-Jishi and G. Dresselhaus, Phys. Rev. B **26**, 4514 (1982).
[8] T. Aizawa, R. Souda, S. Otani, Y. Ishizawa, and C. Oshima, Phys. Rev. B **42**, 11469 (1990).
[9] V. N. Popov, Phys. Rev. B **66**, 153408 (2002).
[10] J. X. Cao, X. H. Yan, Y. Xiao, Y. Tang, and J. W. Ding, Phys. Rev. B **67**, 045413 (2003).
[11] C. Dames *et al.*, Appl. Phys. Lett. **87**, 031901 (2005).
[12] P. Reimann, Phys. Rev. Lett. **86**, 4992 (2001).
[13] S. Denisov, S. Flach, A. A. Ovchinnikov, O. Yevtushenko, and Y. Zolotaryuk, Phys. Rev. E **66**, 041104 (2002).
[14] W. Paul, D. Y. Yoon, and G. D. Smith, J. Chem. Phys. **103**, 1702 (1995).
[15] V. G. Mavrantzas and D. N. Theodorou, Macromolecules **31**, 6310 (1998).
[16] V. A. Harmandaris, V. G. Mavrantzas, and D. N. Theodorou, Macromolecules **31**, 7934 (1998).
[17] J. G. Kirkwood, J. Chem. Phys. **7**, 506 (1939).
[18] K. Pitzer, J. Chem. Phys. **8**, 711 (1940).
[19] L. I. Manevitch and A. V. Savin, Phys. Rev. E **55**, 4713 (1997).
[20] A. V. Savin and L. I. Manevitch, Phys. Rev. B **58**, 11386 (1998).
[21] J. D. Doll and T. L. Beck, J. Chem. Phys. **89**, 5753 (1988).
[22] R. A. Sauerwein and Sabre Kais, Phys. Rev. E **64**, 056120 (2001).
[23] Jian-Sheng Wang, Phys. Rev. Lett. **99**, 160601 (2007).
[24] Dahai He, Sahin Buyukdagli, and Bambi Hu, Phys. Rev. E **78**, 061103 (2008).